Molecular Crystals and Liquid Crystals

Publication details, including instructions for authors and subscription information:
http://www.tandfonline.com/loi/gmcl20

Polarization Resolved Angular Patterns of Light Transmitted Through Nematic Liquid Crystal Cells

A. D. Kiselev [a b], M. S. Soskin [a], I. O. Buinyi [a], R. G. Vovk [a] & V. G. Chigrinov [b]

[a] Institute of Physics of National Academy of Sciences of Ukraine, Kyiv, Ukraine

[b] Hong Kong University of Science and Technology, Kowloon, Hong Kong

Version of record first published: 05 Apr 2011

To cite this article: A. D. Kiselev, M. S. Soskin, I. O. Buinyi, R. G. Vovk & V. G. Chigrinov (2008): Polarization Resolved Angular Patterns of Light Transmitted Through Nematic Liquid Crystal Cells, Molecular Crystals and Liquid Crystals, 494:1, 101-113

To link to this article: http://dx.doi.org/10.1080/15421400802430166

Mol. Cryst. Liq. Cryst., Vol. 494, pp. 101–113, 2008

ISSN: 1542-1406 print/1563-5287 online
DOI: 10.1080/15421400802430166

Polarization Resolved Angular Patterns of Light Transmitted Through Nematic Liquid Crystal Cells

A. D. Kiselev[1,2], M. S. Soskin[1], I. O. Buinyi[1], R. G. Vovk[1], and V. G. Chigrinov[2]
[1]Institute of Physics of National Academy of Sciences of Ukraine, Kyiv, Ukraine
[2]Hong Kong University of Science and Technology, Kowloon, Hong Kong

We study the angular structure of polarization of light transmitted through a nematic liquid crystal cell by analyzing the polarization state as a function of the incidence angles. Theoretical results are obtained by evaluating the Stokes parameters that characterize the polarization of plane waves propagating through the cell at varying direction of incidence. Using the Stokes polarimetry technique we measured the polarization resolved conoscopic patterns emerging after the homeotropically aligned nematic cell illuminated by the convergent light beam. The resulting polarization resolved angular patterns are described in terms of the polarization singularities such as C-points *and* L-lines.

Keywords: nematic liquid crystal; polarization of light; polarization singularities

1. INTRODUCTION

The effect of liquid crystals (LCs) on the polarization of propagating waves is extensively used to obtain the information about their properties. When the LC cell is placed between two crossed polarizers, the anisotropy induced changes of the polarization manifest themselves in variations of the intensity of the transmitted light. This arrangement is typical for a number of experimental methods employed to characterize orientational structures in LC cells. Examples include the crystal rotation technique [1] and the conoscopic measurements

This work was partially supported by CERG grant No. 612406.
Address correspondence to A. D. Kiselev, Institute of Physics of National Academy of Sciences of Ukraine, prospekt Nauky 46, Kyiv 03028, Ukraine. E-mail: kiselev@iop.kiev.ua

of the images formed by a convergent light beam transmitted through an anisotropic material [2]. These conoscopic images describe the angular dependence of light transmittance on the projection plane in experiments with two crossed polarizers.

In this paper we present the results of our investigation into the polarization structure behind the conoscopic images performed by analyzing the polarization state of light transmitted through a nematic liquid crystal (NLC) cell as a function of the incidence angles. We explore the characteristic features of the two-dimensional angular distributions of the Stokes parameters represented by the fields of polarization ellipses in the plane of projection. Such distributions will be referred to as the *polarization resolved angular (conoscopic) patterns* and, in contrast to conventional conoscopic images, provide a complete description of the polarization state.

Polarization distributions are suitably characterized in terms of polarization singularities such as *C-points* at which the light wave is circularly polarized and *L-lines* along which the light polarization is linear [3–5]. We will describe our polarization resolved angular patterns in terms of these polarization singularities representing structurally stable topological defects.

The paper is organized as follows. In Sec. 2 we give experimental details and describe our setup employed to carry out measurements using a suitably modified method of the Stokes polarimetry [6–8]. In Sec. 3 we briefly describe our theoretical approach to the solution of the transmission problem and explain how the results are used to plot the polarization resolved conoscopic patterns. The case of homeotropic structure is detailed in subsection 3.1. Experimentally measured and computed fields of the polarization ellipses are presented in Sec. 4. Our concluding remarks are given in Sec. 5.

2. EXPERIMENT

In our experiments we used the NLC cell of thickness $h = 110\,\mu\text{m}$ filled with the nematic liquid crystal mixture $E7$ from Merk. Two glass substrates were assembled to form a hometropically oriented NLC cell. At the wavelength of light generated by a low power He-Ne laser from Coherent Group with $\lambda = 632.8\,\text{nm}$ (see Fig. 1), the ordinary and extraordinary refractive indices of the NLC are $n_o = 1.5246$ and $n_e = 1.7608$, respectively; the refractive index of the glass substrates is $n_m = 1.5$.

Figure 1 shows our experimental setup devised to perform the conoscopic measurements using the Stokes polarimetry technique [6–8]. The cell is irradiated with a convergent light beam formed by the microscope objective of high numerical aperture L3. The input

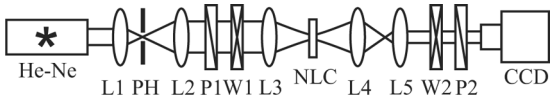

FIGURE 1 Experimental setup: He-Ne is the laser; L1, L2 and L5 are the collimating lenses; L3 and L4 are the microscope objectives; PH is the pinhole; NLC is the NLC cell; P1 and P2 are the polarizers; W1 and W2 are the quarter wave plates; CCD is the CCD camera. A microscope objective L3 is illuminated with an elliptically polarized and expanded parallel beam of light from a He-Ne laser. The output from a second objective L4 is collected by a CCD camera through the Stokes analyzer.

polarizer P1 is combined with the properly oriented quarter wave plate W1 to control the polarization characteristics (the ellipticity and the azimuth of polarization) of a He-Ne laser beam which is expanded and collimated using the lenses L1 and L2. A charge coupled device (CCD) camera collects the output from the microscope objective L4 through the collimating lense L5 and the Stokes analyzer represented by the combination of the quarter wave plate W2 and the polarizer P2.

This optical arrangement therefore collects simultaneously the transmittance of the cell for a range of incident angles. The distribution of the Stokes parameters $S_0 \ldots S_3$ describing the state of polarization of the transmitted light can then be obtained by performing the measurements at six different combinations of the quarter wave plate W2 and the analyzer P2 and using the well-known relations [9]

$$S_1 = I_{0^\circ} - I_{90^\circ}, \quad S_2 = I_{45^\circ} - I_{135^\circ}, \tag{1a}$$

$$S_3 = I_{RCP} - I_{LCP}, \quad S_0 = \sqrt{S_1^2 + S_2^2 + S_3^2}, \tag{1b}$$

where I_{0°, I_{90°, I_{45° and I_{135° are the linearly polarized components (subscript indicates the orientation angle of the analyzer); I_{RCP} and I_{LCP} are the right- and left-handed circularly polarized components measured in the presence of the quarter wave plate W2.

Geometrically, the distribution of the Stokes parameters measured in the observation plane can be conveniently represented by the two-dimensional field of the polarization ellipses. The geometrical elements of polarization ellipses that determine the polarization ellipse field can be readily computed from the Stokes parameters (1).

The orientation of a polarization ellipse is specified by the azimuthal angle of polarization (*polarization azimuth*)

$$\phi_p = \frac{1}{2}\arg(S_1 + iS_2) \tag{2}$$

and its eccentricity is described by the signed ellipticity parameter

$$\varepsilon_{ell} = \tan\left[\frac{1}{2}\arcsin\left(\frac{S_3}{S_0}\right)\right]. \tag{3}$$

This parameter will be referred to as the *ellipticity*. The handedness of the ellipse is determined by the sign of the ellipticity parameter ε_{ell}.

3. THEORY

We consider a NLC cell of thickness h sandwiched between two parallel plates that are normal to the z axis: $z=0$ and $z=h$ (see Fig. 2). The NLC represents a uniaxially anisotropic material characterized by the dielectric tensor [2]

$$\varepsilon_{\alpha\beta} = \varepsilon_\perp \delta_{\alpha\beta} + (\varepsilon_\parallel - \varepsilon_\perp) d_\alpha d_\beta, \quad \alpha, \beta \in \{x, y, z\}, \tag{4}$$

where the unit vector $\hat{\mathbf{d}} = (\sin\theta_d \cos\phi_d, \sin\theta_d \sin\phi_d, \cos\theta_d)$ is the NLC *director* giving the preferential orientation of NLC molecules and directed along the local optical axis. The two principal values of the dielectric tensor, $\varepsilon_\perp$ and $\varepsilon_\parallel$, give the ordinary and extraordinary refractive indices, $n_o = \sqrt{\mu\varepsilon_\perp}$ and $n_e = \sqrt{\mu\varepsilon_\parallel}$, where μ is the NLC magnetic permeability. The medium surrounding the NLC cell

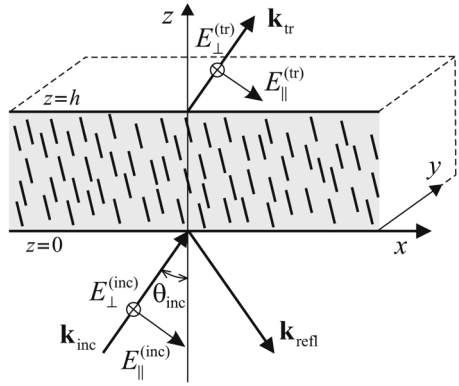

FIGURE 2 Geometry of the NLC cell in the plane of incidence.

is assumed to be optically isotropic and characterized by the dielectric constant ε_m, the magnetic permittivity μ_m and the refractive index $n_m = \sqrt{\mu_m \varepsilon_m}$.

Referring to Figure 2, there are two plane waves in the lower half space $z \leq 0$ bounded by the entrance face of the NLC cell: the incoming incident wave $\{\mathbf{E}_{inc}, \mathbf{H}_{inc}\}$ and the outgoing reflected wave $\{\mathbf{E}_{refl}, \mathbf{H}_{refl}\}$. The transmitted plane wave $\{\mathbf{E}_{tr}, \mathbf{H}_{tr}\}$ is excited by the incident wave and propagates along the direction of incidence in the upper half space $z \geq h$ after the exit face.

The polarization vector of a plane wave traveling in the isotropic ambient medium along the wave vector $\mathbf{k} = k\hat{\mathbf{k}} = k_x\hat{\mathbf{x}} + k_z\hat{\mathbf{z}}$ can be written in the form

$$\mathbf{E}(\hat{\mathbf{k}}) = E_{\parallel}\mathbf{e}_x(\hat{\mathbf{k}}) + E_{\perp}\mathbf{e}_y(\hat{\mathbf{k}}) = E_{+}\mathbf{e}_{+}(\hat{\mathbf{k}}) + E_{-}\mathbf{e}_{-}(\hat{\mathbf{k}}), \tag{5a}$$

$$\mathbf{e}_{\pm}(\hat{\mathbf{k}}) = 2^{-1/2}[\mathbf{e}_x(\hat{\mathbf{k}}) \pm i\mathbf{e}_y(\hat{\mathbf{k}})], \quad E_{\pm} = 2^{-1/2}(E_{\parallel} \pm iE_{\perp}), \tag{5b}$$

$$\mathbf{e}_x(\hat{\mathbf{k}}) = k^{-1}(k_z\hat{\mathbf{x}} - k_x\hat{\mathbf{z}}), \ \mathbf{e}_y(\hat{\mathbf{k}}) = \hat{\mathbf{y}} \tag{5c}$$

Since in our case the transmission problem is linear, the circular components of the transmitted and the incident waves, $\{E_{+}^{(tr)}, E_{-}^{(tr)}\}$ and $\{E_{+}^{(inc)}, E_{-}^{(inc)}\}$ are linked through the linear relation

$$\begin{pmatrix} E_{+}^{(tr)} \\ E_{-}^{(tr)} \end{pmatrix} = \mathbf{T}_c \begin{pmatrix} E_{+}^{(inc)} \\ E_{-}^{(inc)} \end{pmatrix} \tag{6}$$

where $\mathbf{T}_c$ is the *transmission (transfer) matrix*. The exact expression for the transmission matrix of the NLC cell with arbitrary oriented director was obtained in [10] using the 4×4 matrix formalism [11] combined with the orthogonality relations [12].

The transmission matrix is a function of the incidence angle θ_{inc} (see Fig. 2) and the azimuthal angle of incidence ϕ_{inc} that determines orientation of the plane of incidence. So, the matrix

$$\hat{\mathbf{T}}(\rho, \phi) = \exp(-i\phi\sigma_3)\ \mathbf{T}_c(\rho, \phi_d - \phi)\exp(i\phi\sigma_3), \quad \sigma_3 = diag(1, -1) \tag{7}$$

describes the angular patterns in the transverse plane of projection where the polar coordinates, ρ and ϕ, are

$$\rho = r\tan\theta_{inc}, \ \phi = \phi_{inc} \tag{8}$$

and the Cartesian coordinates, $x = \rho\cos\phi$ and $y = \rho\sin\phi$, are proportional to the aperture dependent scale factor r.

The relation (8) establishes a one-to-one correspondence between the incidence angles and the points in the observation plane. Given

the angles, the Stokes parameters

$$S_1 = 2\,\mathrm{Re}(E_+^* E_-), \quad S_2 = 2\,\mathrm{Im}(E_+^* E_-), \tag{9a}$$

$$S_3 = |E_+|^2 - |E_-|^2, \quad S_0 = |E_+|^2 + |E_-|^2 \tag{9b}$$

can be combined with Equations (2) and (3) to evaluate the polarization azimuth ϕ_p and the ellipticity parameter ε_{ell} characterizing the polarization ellipse (the state of polarization) of the transmitted wave at the corresponding point of the plane. This procedure yields the two-dimensional field of polarization ellipses.

The *C-points* can be regarded as the phase singularities of the complex Stokes field

$$S = S_1 + iS_2 \tag{10}$$

that vanishes provided $S_1 = S_2 = 0$ and the polarization is circular. Such singularities are characterized by the winding number which is the signed number of rotations of the two-component field (S_1, S_2) around the circuit surrounding the singularity [13]. The winding number also known as the signed strength of the dislocation is generically ± 1.

Since the polarization azimuth (2) is defined modulo π and $2\phi_p = \arg S$, the dislocation strength is twice the index of the corresponding *C-point*, I_C. For generic *C-points*, $I_C = \pm 1/2$ and the index can be computed from the formula

$$I_C = \frac{1}{2} sign[\mathrm{Im}(\partial_x S^* \partial_y S)]_{\substack{x=x_C \\ y=y_C}}, \tag{11}$$

where $\partial_x f$ is the partial derivative of f with respect to x, x_C and y_C are the coordinates of the *C-point*.

L-lines are the curves of linear polarization where $S_3 = 0$ and the polarization handedness is undefined.

3.1. Homeotropic Cell

Now we concentrate on the special case in which the NLC director $\hat{\mathbf{d}}$ is parallel to the z axis $\theta_d = 0\,\mathrm{deg}$ and the orientational structure is homeotropic. The elements of the transmission matrix are [10]

$$\mathbf{T}_C = \begin{pmatrix} t_e + t_o & t_e - t_o \\ t_e - t_o & t_e + t_o \end{pmatrix}, \quad t_{e,o} = \mu_m n_m^{-1} \cos\theta_{inc} \tau_{e,o}^{-1}. \tag{12}$$

$$\tau_e = 2\mu_m n_m^{-1}\cos\theta_{inc}\cos\delta_e - i\left[q_z^{(e)}\right]^{-1}\sin\delta_e[(\mu_m n_o n_m^{-1}\cos\theta_{inc})^2 + (n_o^{-1}q_z^{(e)})^2], \tag{13a}$$

$$\tau_o = 2\mu_m n_m^{-1}\cos\theta_{inc}\cos\delta_o - i\left[q_z^{(o)}\right]^{-1}\sin\delta_o[\cos^2\theta_{inc} + (\mu_m n_m^{-1}q_z^{(o)})^2], \tag{13b}$$

where is $q_z^{(o)} = \sqrt{n_o^2 - n_m^2\sin^2\theta_{inc}}$, $q_z^{(e)} = n_o n_e^{-1}\sqrt{n_e^2 - n_m^2\sin^2\theta_{inc}}$, $\delta_{o,e} = q_z^{(o,e)}k_{vac}h$ and k_{vac} the free-space wave number.

When the incident light is elliptically polarized, the circular components of the electric field can be expressed in terms of the azimuthal angle of polarization ψ_p and the ellipticity parameter ε as follows

$$E_\nu^{(inc)} = \frac{a_\nu}{\sqrt{2}}\exp(-i\nu\psi_p)|E_{inc}|, \quad a_\nu = \frac{1+\nu\varepsilon}{\sqrt{1+\varepsilon^2}}, \quad \nu \in \{+,-\}. \tag{14}$$

Using the matrix (7) we derive the expression for the reduced components of the transmitted wave

$$\frac{E_\nu^{(tr)}}{|E_{inc}|} \equiv \frac{\Psi_\nu}{2\sqrt{2}} = [a_\nu(t_e + t_o) + a_{-\nu}(t_e - t_o)\exp(-2i\nu\psi)]\exp(-i\nu\psi_p), \tag{15}$$

where $\psi = \phi - \psi_p$. From Eqs. (9) and (15) it can be seen that, owing to the cylindrical symmetry of the homeotropic structure, the Stokes parameters of the transmitted wave depend only on the difference of the azimuthal angles $\psi = \phi - \psi_p$. Thus the sole effect of changing the polarization azimuth of the incident wave is the rotation of the polarization ellipse field.

The *C-point* in the observation plane where $|E_\nu^{(tr)}| = 0$ and $\varepsilon = -\nu$ might be called the *C_ν-point*. The polar coordinates of the *C_ν-point* can be found by solving the equation

$$|\Psi_\nu(\rho,\phi)| = 0 \tag{16}$$

that generally has multiple solutions, $\rho_k^{(\nu)}$ and $\phi_k^{(\nu)}$, labeled by the integer k.

The incidence angles of the *C_ν-point*, $\rho = \rho_k^{(\nu)}$, can be conveniently obtained from the condition $a_\nu^2|t_e + t_o|^2 = a_{-\nu}^2|t_e - t_o|^2$ [see Eq. (15)] written in the following form

$$-\nu F(\rho) \equiv -\nu\frac{2R(\rho)}{|t|^2} = \gamma(\varepsilon), \tag{17}$$

$$R(\rho) = \mathrm{Re}(t_e t_o^*) = |t_e||t_o|\cos\delta,\ |t|^2 = |t_e|^2 + |t_o|^2,\ \gamma(\xi) = \frac{2\varepsilon}{1+\varepsilon^2}, \quad (18)$$

where δ is the phase difference. Given the radius (the incidence angle) $\rho = \rho_k^{(\nu)}$, there is a pair of the *C_ν-point* in the circle of this radius with the azimuthal angles given by

$$\phi_k^{(\nu)} = \psi_p \pm \frac{\pi}{2} + \frac{\nu}{2}(\alpha_+ + \alpha_-), \quad (19)$$

$$\tan\alpha_\pm = \frac{Q(\rho_k^{(\nu)})}{|t_e|^2 \pm R(\rho_k^{(\nu)})}, \quad \tan(\alpha_+ + \alpha_-) = \frac{2Q(\rho_k^{(\nu)})}{|t_e|^2 - |t_o|^2}, \quad (20)$$

where $Q(\rho) = \mathrm{Im}(t_e t_o^*) = |t_e||t_o|\sin\delta$.

In the limiting case where the incident light is circularly polarized with $\varepsilon = \pm 1$, the *C-points* develop provided that the condition of isotropy for the transmission coefficients $t_e = \pm t_o$ is satisfied. From Equation (13) we have $t_e = t_o$ for the case of normal incidence with $\rho = 0$, $(\sin\theta_{inc} = 0)$ and the corresponding *C-point* is located at the origin. The isotropy condition $t_e = \pm t_o$ cannot generally be satisfied at oblique incidence and, typically, the *C-point* at the origin is unique.

The graphical solution of Equations (17) is illustrated in Figure 3. Each intersection of the horizontal straight line $\gamma(\varepsilon)$ with the curve $\pm F(\rho)$ determines the radius of the circle containing a pair of the symmetrically arranged *$C\pm$-points*. When the ellipticity parameter ε varies the horizontal line $\gamma(\varepsilon)$ moves vertically changing the location

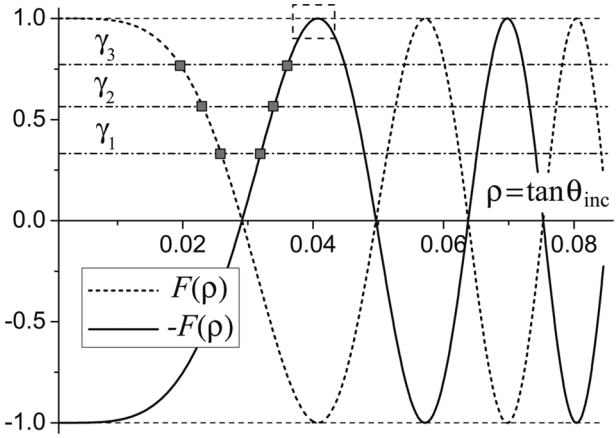

FIGURE 3 Graphical solution of Eq. (17): $n_o = 1.5246$, $n_e = 1.7608$ (NLC E7), $h = 110\,\mu\mathrm{m}$, $n_m = 1.5$.

and the number of the intersection points that describe the radii of the *C-points*.

The general expression for the index of the C_ν-*point* (11) can be recast into the form [10]

$$I_C = \frac{\nu}{2} sign[\mathrm{Im}(\partial_x \Psi_\nu \partial_y \Psi_\nu^*)]_{\substack{x=x_k^{(\nu)} \\ y=y_k^{(\nu)}}} = \frac{\nu}{2} sign[\mathrm{Im}(\partial_\rho \Psi_\nu \partial_\phi \Psi_\nu^*)]_{\substack{\rho=\rho_k^{(\nu)} \\ \phi=\phi_k^{(\nu)}}}. \quad (21)$$

We can now substitute Equation (15) into Equation (21) to derive the result

$$I_C = -\frac{1}{2} sign[\partial_p F(\rho)|_{\rho=\rho_k}]. \quad (22)$$

An important consequence of Equation (22) is that the indicies of the neighbouring *C-points* are opposite in sign.

According to the line classification initially studied in the context of umbilic points [14], for generic *C-points*, the number of the straight lines N_C terminating on singularity, may either be 1 or 3. There are three morphological types of *C-points* [3]. The *C-points* are called the *stars* if the index equals $1/2$ and $NC = 3$. At $I_C = 1/2$, there are two characteristic patterns of polarization ellipses around a *C-point*: the *lemon* with $NC = 1$ and the *monster* with $NC = 3$. Different quantitative criteria to distinguish between the *C-points* of the *lemon* and the *monstar* types are discussed in [15,10].

The transmitted wave is linearly polarized when the condition

$$|\Psi_+(\rho,\ \phi)| = |\Psi_-(\rho,\ \phi)|, \quad (23)$$

is satisfied. So, the equation for the *L-lines* is

$$(1 - \varepsilon^2) Q(\rho) \sin(2\psi) = 4\varepsilon R(\rho) \quad (24)$$

At $\varepsilon = 0$, there are two straight lines of linear polarization: $\phi = \psi_p$ and $\phi = \psi_p + \pi/2$. Other *L-lines* are circles which radii can be found by solving the equation $Q(\rho) = 0$.

The case of linear polarization is, however, structurally unstable and, for elliptically polarized incident waves with $\varepsilon \neq 0$, there is a family of non-intersecting closed *L-lines* bounding the regions of right- and left-handed polarization. At $\varepsilon = \pm 1$, these closed curves become circles with the radii given by the solutions of the equation $R(\rho) = 0$.

4. RESULTS

We can now present both the experimentally measured and computed polarization resolved conoscopic patterns for the NLC cells. These

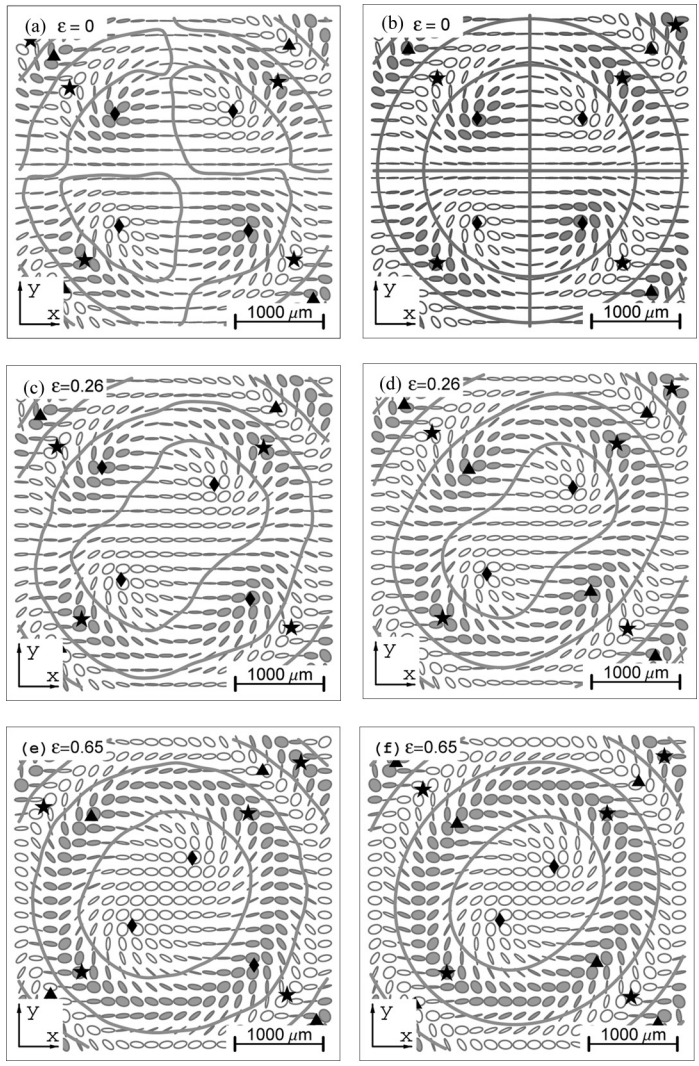

FIGURE 4 Polarization resolved conoscopic patterns for the homeotropically oriented NLC cell, measured (a, c, e) and computed (b, d, f) in the projection plane. The incident light of the wavelength 632.8 nm is polarized with the ellipticity parameter ε and polarization azimuth $\phi_p = 0$. The cell thickness is $h = 110\,\mu$m, $n_o = 1.5246$, $n_e = 1.7608$. The *C-points* of the *star*, the *lemon* and the *monstar* types are marked by stars, diamonds and triangles, respectively. *L-lines* are represented by solid lines. Left-handed and right-handed polarization is respectively indicated by filled and open ellipses.

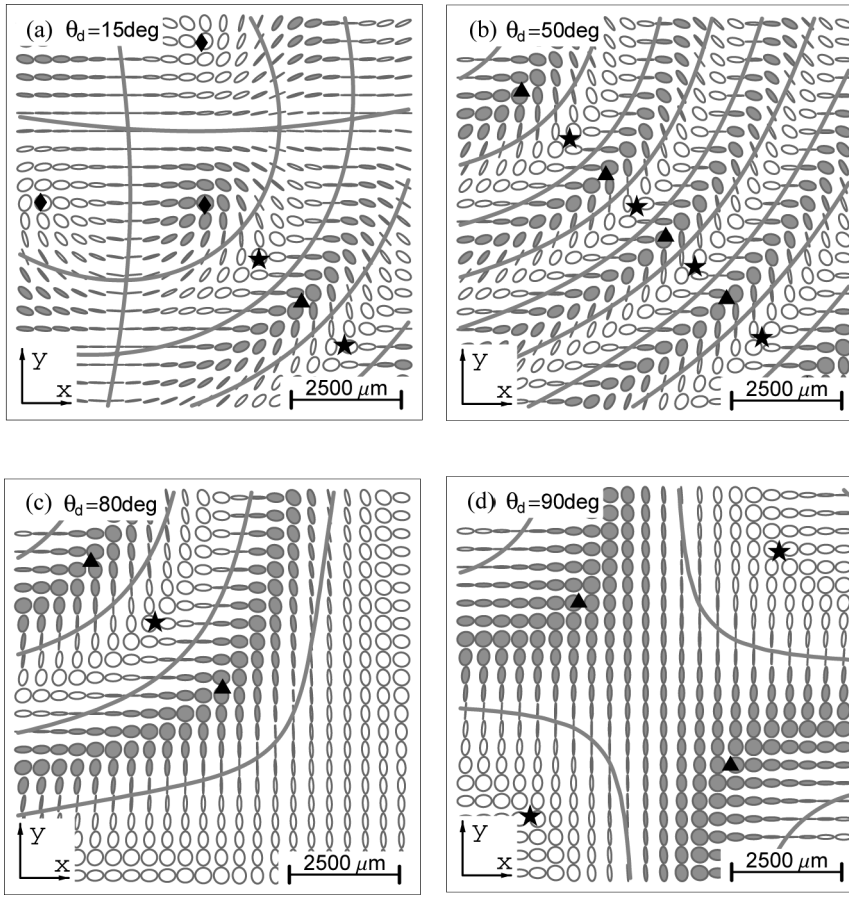

FIGURE 5 Polarization resolved conoscopic patterns for (a–c) tilted and (d) planar orientational structures. The incident light of the wavelength 632.8 nm is linearly polarized at $\phi_p = 0$. The cell thickness is $h = 18.7\,\mu$m, $n_o = 1.527$, $n_e = 1.7102$, $\phi_p = 135$ deg.

patterns are shown as the fields of polarization ellipses in the observation plane with the polar coordinates defined in Equation (8). In our calculations the aperture dependent scale factor r was taken to be 6.3 mm. We also assume that changes of light polarization at the air-glass boundaries are negligible.

Figure 4 presents the results for homeotropically oriented NLC cell. Polarization patterns are measured and computed at three different values of the incident light ellipticity ε. The *C-points* are shown to be arranged in chains formed by four rays along which they alternate

in sign of the handedness and of the index. The *L-lines* are the curves separating the regions of different polarization handedness. It can also be seen that the predictions of the theory are in good agreement with the experimental data.

Referring to Figure 4, the *C-points* move along the radial direction provided the magnitude of the ellipticity parameter $|\varepsilon|$ is not in the immediate vicinity of unity. From Eqs. (19) and (20) it can be seen that the azimuthal angle varies only negligibly.

Computed polarization resolved conoscopic patterns for the tilted and planar NLC configuration are shown in Figure 5. From Figure 5(a) it is seen that, at small tilt angles, the symmetry breaking terms result in the shift of the symmetry center. When the tilt angle angle increases further, the center of symmetry eventually leaves the region specified by the aperture leading to the single-chain structure of the *C-points* shown in Figure 5(b).

In the case of the planar structure with $d_z = 0$ ($\theta_d = 90$ deg), similar to the homeotropic cell, the origin is the symmetry center for the polarization pattern. By contrast to the homeotropic structure, where the polarization field is of the elliptic type, the angular pattern of polarization is of the hyperbolic type for the planar structure [see Fig. 5(d)].

5. CONCLUSIONS

In this paper we have studied the polarization resolved angular patterns of light transmitted through the NLC cell. These patterns can be conveniently represented as fields of polarization ellipses and characterize the polarization structure behind the conoscopic images measured in experiments with two crossed polarizers.

Experimentally, the polarization resolved conoscopic patterns are investigated using a suitably modified method of the Stokes polarimetry designed for accurate measurements of the Stokes parameters [6–8]. For the homeotropically aligned NLC cell we have measured the Stokes distributions at different values of the incident light ellipticity and found that the corresponding fields of the polarization ellipses are in good agreement with the patterns computed using the exact result for the transmission matrix [10].

The theory was applied to characterize the polarization resolved angular patterns in terms of the polarization singularities. After computing loci of the *C-points* and the *L-lines*, we have deduced a simple formula for the index of the *C-points* (22). Interestingly, the polarization singularities appear to be sensitive to the ellipticity parameter of

the incident light ε. For elliptically polarized incident waves, there is a chain-like structure of four radial rays with the *C-points* alternating in sign of the handedness and of the index.

We have also computed polarization resolved conoscopic patterns for tilted and planar NLC configurations. The tilt angle was found to have a considerable effect on the chain-like structure of the *C-points*.

REFERENCES

[1] Baur, G., Wittwer, V., & Berreman, D. W. (1976). *Phys. Lett. A*, *56*, 142.
[2] de Gennes, P. G. & Prost, J. (1993). *The Physics of Liquid Crystals*, Clarendon Press: Oxford.
[3] Nye, J. F. (1983). *Proc. R. Soc. Lond. A*, *389*, 279–290.
[4] Nye, J. F. & Hajnal, J. V. (1987). *Proc. R. Soc. Lond. A*, *409*, 21–36.
[5] Nye, J. F. (1999). *Natural Focusing and Fine Structure of Light: Caustics and Wave Dislocations*, Institute of Physics Publishing: Bristol.
[6] Soskin, M. S., Denisenko, V., & Freund, I. (2003). *Opt. Lett.*, *28*(16), 1475–1477.
[7] Soskin, M. S., Denisenko, V., & Egorov, R. (2004). *J. Opt. A: Pure Appl. Opt.*, *6*, S281–S287.
[8] Flossmann, F., Schwarz, U. T., & Dennis, M. R. (2005). *Phys. Rev. Lett.*, *95*, 253901.
[9] Born, M. & Wolf, E. (1999). *Principles of Optics*, Cambridge Unversity Press: Cambridge.
[10] Kiselev, A. D. (2007). *J. Phys.: Condens. Matter*, *19*(24), 246102.
[11] Berreman, D. W. (1972). *J. Opt. Soc. Am.*, *62*, 502–510.
[12] Oldano, C. (1989). *Phys. Rev. A*, *40*(10), 6014–6020.
[13] Mermin, N. D. (1979). *Rev. Mod. Phys.*, *51*, 591–648.
[14] Berry, M. V. & Hannay, J. H. (1977). *J. Phys. A.: Math. Gen.*, *10*(11), 1809–1821.
[15] Dennis, M. R. (2002). *Opt. Commun.*, *213*, 201–221.